

# RADIATIVE TRANSFER IN HIGHLY SCATTERING MATERIALS--NUMERICAL SOLUTION AND EVALUATION OF APPROXIMATE ANALYTIC SOLUTIONS

Kenneth C. Weston\*, Albert C. Reynolds, Jr.†  
Arif Alikhan\* and Daniel W. Drago\*

The University of Tulsa, Tulsa, Oklahoma 74104

## ABSTRACT

Numerical solutions for radiative transport in a class of anisotropically scattering materials are presented. Conditions for convergence and divergence of the iterative method are given and supported by computed results. The relation of two flux theories to the equation of radiative transfer for isotropic scattering is discussed. The adequacy of the two flux approach for the reflectance, radiative flux and radiative flux divergence of highly scattering media is evaluated with respect to solutions of the radiative transfer equation.

The authors gratefully acknowledge support of this work under NASA Grant NGR-37-008-003. The senior author wishes to express his appreciation to Phillip R. Nachtsheim and John T. Howe of NASA Ames Research Center and to Richard W. Nelson of the Institute of Paper Chemistry for helpful discussions.

- \* Associate Professor. Member AIAA
- † Assistant Professor
- \* Research Assistants



(NASA-CR-139408) RADIATIVE TRANSFER IN  
HIGHLY SCATTERING MATERIALS - NUMERICAL  
SOLUTION AND EVALUATION OF APPROXIMATE  
ANALYTIC SOLUTIONS (Tulsa Univ.) 28 p  
HC \$4.50

CSCL 11D G3/18

Unclass  
54915

N74-30008

## INTRODUCTION

Radiative transport theories involving multiple scattering play an important role in the engineering analysis and simulation of the performance of diathermanous materials. Highly scattering dielectric materials have been proposed, for instance, for the entry heat protection of planetary probes [1]. Other applications include the evaluation of the reflectance of condensed deposits on cryogenic storage tanks [2] and the engineering analysis of opacity in the paint and paper industry [3]. Regardless of the application, engineering approximations of radiative transport continue to be employed despite the increasing ease of computer modeling. Accordingly, this work attempts to provide a unified discussion of the radiative characteristics of anisotropically scattering volume reflectors through new numerical solutions of the equations of radiative transfer, to evaluate several approximations for parameters of importance in thermal analysis, and to clarify the ties which exist between the equation of radiative transport and the approximate theories.

Of primary interest here is the investigation of the radiative energy transport characteristics of volume-reflecting heat shields for hypervelocity entry. In this application a highly scattering, weakly absorbing dielectric material mounted on an opaque, structural substrate is irradiated by an intense, diffuse radiative flux. Low absorption allows the incident radiation to penetrate in depth with limited conversion of radiative to thermal energy. In addition, high scattering provides an internal mechanism for spatially distributed reversal of the direction of the incident radiation. In this way, dielectrics are capable of reflecting intense incident radiative fluxes efficiently while convective heating is also handled efficiently through ablation mechanisms.

Multiple scattering studies including effects of anisotropy have focused in the past on the reflectance, transmittance, and emittance of plane-parallel layers exposed to parallel incident irradiation [4,5,6]. Solutions of the transfer equation presented here assume a diffuse, incident intensity field appropriate to the entry vehicle application. With this orientation, emphasis is placed on thermal analysis parameters and their approximation.

The approximations considered for isotropic scattering stem from the Schuster-Schwarzschild [7] and Kubelka-Munk [8] two-flux models. Exact solutions of the two-flux equations as well as approximations [9] and a reinterpretation [10] are evaluated in relation to radiative transfer equation solutions. An earlier evaluation of the Schuster-Schwarzschild model [11] considered coupled radiative and conductive energy transport in a broader context whereas the present study focuses on the uncoupled, high albedo problem.

## ANALYSIS

### Transfer Equation Formulation

The Equation of Radiative Transfer is considered to govern the transport of radiation in dielectric media. Polarization effects are known to be negligible in thermal problems involving multiple scattering [12], and are therefore not considered. A diffuse, gray radiative flux is assumed. The medium is assumed to be isothermal, to be gray, to have unity index of refraction and to have uniform absorption and scattering coefficients. The rear boundary is opaque and reflects specularly with constant reflectance  $R_B$ .

In order to evaluate the influence of anisotropic scattering, a phase function of the form  $P(\Theta) = \omega(1 + x \cos \Theta)$  is assumed [6]. Here  $\omega$  is the albedo,  $\Theta$  is the

angle between incoming and scattered beams at a point in the medium; and  $x$  is an anisotropy parameter which provides backward scattering ( $-1.0 \leq x < 0$ ), isotropic scattering ( $x = 0$ ), and forward scattering ( $0 < x \leq 1.0$ ).

The intensity field is azimuthally symmetric in this plane-parallel case and may be represented by  $I(\tau, \mu)$  where  $\mu$  is the cosine of the angle between an arbitrary beam and the inward normal to the medium boundary and  $\tau$  is the optical depth measured from the incident flux boundary. The transfer equation is:

$$\mu \frac{dI(\tau, \mu)}{d\tau} = -I(\tau, \mu) + \frac{1}{4\pi} \int_{-1}^1 \int_0^{2\pi} p(\mu, \theta, \underline{\mu}, \underline{\theta}) I(\tau, \underline{\mu}) d\underline{\mu} d\underline{\theta} + (1-\omega) I_{BB} \quad (1)$$

where in spherical coordinates  $P(\Theta)$  becomes:

$$P(\mu, \theta, \underline{\mu}, \underline{\theta}) = \omega \left\{ 1 + x [\mu \underline{\mu} + (1-\mu^2)^{1/2} (1-\underline{\mu}^2)^{1/2} \cos(\theta - \underline{\theta})] \right\} \quad (2)$$

Substituting (2) into (1) and integrating with respect to  $\underline{\theta}$  yields the transfer equation:

$$\mu \frac{dI(\tau, \mu)}{d\tau} = -I(\tau, \mu) + \frac{\omega}{2} \int_{-1}^1 (1 + x \mu \underline{\mu}) I(\tau, \underline{\mu}) d\underline{\mu} + (1-\omega) I_{BB} \quad (3a)$$

Evaluating the integral of (3a) via Gaussian quadrature gives:

$$\mu_i \frac{dI}{d\tau}(\tau, \mu_i) \cong -I(\tau, \mu_i) + \frac{\omega}{2} \sum_{j=-k}^k a_j (1 + x \mu_i \mu_j) I(\tau, \mu_j) + (1-\omega) I_{BB} \quad (3b)$$

where the  $a_j$ 's are the Gaussian weights, the  $\mu_j$ 's specify the Gaussian directions, and  $k$  is the order of the Gaussian quadrature. In (3b)  $a_{-j} = a_j$  and  $\mu_{-j} = -\mu_j$ . Boundary conditions for the transfer equation are given by a specified diffuse intensity field at  $\tau = 0$  and specular reflection at the boundary  $\tau = \tau_0$  given by:

$$I(\tau_0, \mu_{-j}) = R_B I(\tau_0, \mu_j) + (1-R_B) I_{BB}(\tau_0) \quad (4)$$

where  $R_B$  is the reflectance of the medium-substrate interface.

For purposes of evaluation of approximate theories discussed below, right and left directed half fluxes and net radiative flux are defined in terms of the transfer equation solution field  $I(\tau, \mu)$  as:

$$q^+(\tau) = 2\pi \int_0^1 I(\tau, \mu) \mu d\mu \approx 2\pi \sum_{i=1}^k a_i \mu_i I(\tau, \mu_i) \quad (5a)$$

$$q^-(\tau) = 2\pi \int_0^{-1} I(\tau, \mu) \mu d\mu \approx -2\pi \sum_{i=-k}^{-1} a_i \mu_i I(\tau, \mu_i) \quad (5b)$$

$$q(\tau) = 2\pi \int_{-1}^1 I(\tau, \mu) \mu d\mu = q^+ - q^- \quad (6)$$

Of prime importance in the calculation of the temperature field due to radiative absorption is the divergence of the radiative flux which in the plane-parallel case is proportional to the derivative  $dq/d\tau$ . In order to avoid numerical differentiation an exact expression for  $dq/d\tau$  may be obtained by integration of the transfer equation (3a) over the entire solid angle. The resulting expression is:

$$\frac{dq}{d\tau}(\tau) = -2\pi (1-\omega) \int_{-1}^1 I(\tau, \mu) d\mu + 4\pi (1-\omega) I_{BB} \approx -2\pi (1-\omega) \sum_{i=-k}^k a_i I(\tau, \mu_i) + 4\pi (1-\omega) I_{BB} \quad (7)$$

It is evident from equations (5), (6) and (7) that the radiative flux and radiative flux divergence expressions do not depend explicitly on the anisotropy parameter. Thus anisotropy influences those quantities only through the intensity field. Reflectance may be determined when the intensity field at the left boundary is known. The hemispherical-directional reflectance and hemispherical reflectance are:

$$R_{H-D}(\mu_{-j}) = \pi I(0, \mu_{-j}) / q^+(0), \quad R = q^-(0) / q^+(0) \quad (8a, b)$$

### Numerical Solution of the Radiative Transfer Equation

Replacing the derivative in (3b) by a forward difference quotient for  $\mu_i > 0$  and a backward difference quotient for  $\mu_i < 0$  yields the set of equations:

$$I(\tau + \Delta\tau, \mu_i) = [1 - (\Delta\tau / \mu_i)] I(\tau, \mu_i) + [\omega \Delta\tau / 2 \mu_i] \sum_{i=-k}^k a_i (1 + x \mu_i \mu_i) I(\tau, \mu_i) \\ + [(1 - \omega) \Delta\tau / \mu_i] I_{BB} \quad \text{for } \mu_i > 0 \quad (9a)$$

$$I(\tau - \Delta\tau, \mu_i) = [1 - (\Delta\tau / |\mu_i|)] I(\tau, \mu_i) + [\omega \Delta\tau / 2 |\mu_i|] \sum_{i=-k}^k a_i (1 + x \mu_i \mu_i) I(\tau, \mu_i) \\ + [(1 - \omega) \Delta\tau / |\mu_i|] I_{BB} \quad \text{for } \mu_i < 0 \quad (9b)$$

When an initial approximation to the radiation field is known and left boundary incident intensities are specified, equation (9a) can be used to compute the right directed intensities at successive nodal points. When the march from  $\tau = 0$  to  $\tau = \tau_0$  is complete, that is, when all right-directed intensities have been computed, the rear surface boundary condition provides values for  $I(\tau_0, \mu_{-j})$ . Equation (9b) is then used to march back to the incident flux boundary. The initial intensity field approximation is then replaced by this newly computed field and a second iteration is performed. In practice the iteration procedure is continued until two successive iterates for the intensity field differ by less than a specified tolerance. A similar procedure was employed in reference [13].

Equations (9a) and 9b) together with the appropriate boundary conditions can be written in a matrix vector equation of the form  $I = MI + C$  where  $I$  is a vector which has as its components the intensities in all directions at all nodes,  $M$  is a coefficient matrix, and  $C$  is a known vector determined from the specified boundary data and the values of  $[(1 - \omega) \Delta\tau / |\mu_i|] I_{BB}$ . This iterative procedure can be written:

$$I^{(k+1)} = M I^{(k)} + C \quad \text{for } k = 0, 1, 2, \dots \quad (10)$$

where  $I^{(0)}$  is the initial approximation to the intensity field. It is well known, [14], that the iterative scheme (10) is convergent if and only if  $\rho(M) < 1$  where  $\rho(M)$  denotes the spectral radius of the matrix  $M$ . In the case of isotropic scattering if:

$$\frac{\Delta\tau}{|\mu_i|} = \frac{\tau_0}{|\mu_i| (N-1)} \leq \frac{1}{1 - (a_i \omega / 2)} \quad \text{for all } i \quad (11)$$

where  $N$  is the number of nodes in the finite difference approximation, it can be shown that  $\|M\|_{\infty} < 1$  where  $\|M\|_{\infty}$  denotes the infinity norm of the matrix  $M$ . Since  $\rho(M) \leq \|M\|_{\infty}$ , [14], if condition (11) is satisfied, convergence of the iteration procedure (10) is guaranteed. It is interesting to note that condition (11) is satisfied if and only if the coefficient of  $I(\tau, \mu_i)$  in (9) is non-negative. The convergence boundary given by (11) is shown in Figure 1 as related to quadrature order. For all cases attempted within this convergence boundary, smooth convergent solutions were obtained. However, it is possible to obtain convergent solutions in cases where condition (11) is not satisfied. These solutions are characterized by oscillatory irregularities in intensity near the physical boundaries and in directions closest to parallel to the boundaries. On the other hand calculations performed for  $\omega = .9995$  and  $(\Delta\tau / \min|\mu_i|)$  greater than about 2.0 diverged rapidly. For first order Gaussian quadrature, it can be shown analytically that the method will diverge if  $(\Delta\tau / |\mu_i|) > (2.0/\omega)$ . While only a limited number of runs were made for optical thicknesses other than 3.177 and albedos other than .9995,  $(\Delta\tau / \min|\mu_i|) > (2.0/\omega)$  appears to be sufficient condition for divergence. It is worthwhile to remark that the iteration procedure converges more rapidly when newly obtained intensity values are used as soon as they are generated. This is not surprising since using new intensity values as soon as they are available is analogous to changing from a Jacobi type iterative procedure to a Gauss-Seidel procedure.

In order to verify the accuracy of the iteration technique a computation made with the iterative technique was compared with an available unpublished solution obtained by the matrix eigenvector technique of [15]. The resulting intensity field using fourth order Gaussian quadrature and 21 nodes is shown in Figure 2. The solution corresponds to radiative transfer between two black boundaries through a nonabsorbing isotropically scattering medium

( $\omega = 1.0$ ) where the left boundary and medium are at  $1111^\circ\text{K}$  and the right boundary is at  $555.5^\circ\text{K}$ . The intensity fields are seen to be in good detailed agreement within about 1%. This is within the maximum error claimed in reference [15]. For most of the calculations presented here the order of quadrature was increased to eighth and the number of nodes to at least 101.

### Approximate Methods

The approximate methods for radiative transfer considered stem from two-flux models which have found wide application. Models for isotropic scattering only are considered. These models may be related to each other and to the equation of radiative transfer discussed above. A link between the transfer equation and the two-flux relations known as the Schuster-Schwarzschild equations, reference [7], may be established by assuming that the intensity field is fully described by two functions of optical depth only:

$$I(\tau, \mu) = \begin{cases} I^+(\tau), & \mu > 0 \\ I^-(\tau), & \mu < 0 \end{cases} \quad (12)$$

Here  $I^+$  represents the value of the directionally independent intensity of rays traversing the medium from the incident flux boundary toward the rear ( $\tau$  increasing), and  $I^-$  similarly represents those rays proceeding forward from the rear ( $\tau$  decreasing). Introducing these restrictions and separately integrating the transfer equation over the half spaces  $\mu > 0$  and  $\mu < 0$ , the differential equations:

$$(1/2)(dI^+/d\tau) = -I^+ + (\omega/2)(I^+ + I^-) + (1-\omega) I_{BB} \quad (13a)$$

$$-(1/2)(dI^-/d\tau) = -I^- + (\omega/2)(I^+ + I^-) + (1-\omega) I_{BB} \quad (13b)$$

are obtained. These are the Schuster-Schwarzschild equations obtained in reference [7] in a slightly more general context. The half fluxes and net radiative flux are

easily related to the intensities  $I^+$  and  $I^-$  using equations (4) and (5):

$$q^+(\tau) = 2\pi \int_0^1 I^+(\tau) \mu d\mu = \pi I^+(\tau) \quad (14a)$$

$$q^-(\tau) = 2\pi \int_0^{-1} I^-(\tau) \mu d\mu = \pi I^-(\tau) \quad (14b)$$

$$q = 2\pi \int_{-1}^1 I(\tau, \mu) \mu d\mu = q^+(\tau) - q^-(\tau) = \pi [I^+(\tau) - I^-(\tau)] \quad (14c)$$

Using equations (13) and (14) the Schuster-Schwarzschild equations may be expressed in terms of the half-fluxes as:

$$(dq^+/d\tau) = (\omega - 2) q^+ + \omega q^- + 2\pi (1 - \omega) I_{BB} \quad (15a)$$

$$-(dq^-/d\tau) = (\omega - 2) q^- + \omega q^+ + 2\pi (1 - \omega) I_{BB} \quad (15b)$$

Equations (15) are the isotropic form of the transport equations given by Bergquam and Seban [11]. In reference [11], equations (15) together with an energy equation were solved iteratively on a digital computer to evaluate the two flux method for emission-coupled cases.

The albedo  $\omega$  and optical thickness  $\tau$  have similar interpretations in the equation of radiative transfer and in the Schuster-Schwarzschild equations. It is well known that these quantities may be related to constant scattering, absorption and extinction coefficients  $S$ ,  $K$  and  $\beta$  through

$$\tau = \beta y, \quad \beta = S + K, \quad \omega = \frac{S}{S + K} \quad (16a, b, c)$$

where  $y$  is the physical depth measured from the incident flux boundary. It is through these coefficients that direct associations may be made with another two-flux model to be discussed later. Transforming the independent variable in equations (15) to  $y$  and introducing the scattering and absorption coefficients, the Schuster-Schwarzschild equations become:

$$(dq^+/dy) = -(2K + S) q^+ + S q^- + 2\pi K I_{BB} \quad (17a)$$

$$-(dq^-/dy) = -(2K + S) q^- + S q^+ + 2\pi K I_{BB} \quad (17b)$$

An entirely separate tradition in two-flux radiation field analysis has developed in the paint and paper industry. The basic equations attributed to Kubelka and Munk [8] may also be formulated in terms of half fluxes  $q^+$  and  $q^-$  and the physical depth  $y$ . These equations, however, include independently defined scattering and absorption coefficients  $s$  and  $k$ . The equations are formulated by requiring that each half flux be augmented by scattering from the opposing half flux and by emission, and be diminished by scattering to the opposing half flux and by absorption. The Kubelka-Munk differential equations are:

$$(dq^+/dy) = -(s + k) q^+ + s q^- + \pi k I_{BB} \quad (18a)$$

$$(dq^-/dy) = (s + k) q^- - s q^+ - \pi k I_{BB} \quad (18b)$$

Comparison of equations (17) and (18) shows that the simple relations:

$$s = S, \quad k = 2K \quad (19a,b)$$

allow association of the Kubelka-Munk equations with the Schuster-Schwarzschild equations and hence with the equation of radiative transport. The optical depth and albedo may then be related to the Kubelka-Munk coefficients through:

$$\omega = \frac{2s}{2s + k}, \quad \tau = (s + \frac{k}{2}) y \quad (20a,b)$$

While the association of the Kubelka-Munk equations with the Schuster-Schwarzschild and radiative transfer equations discussed above is satisfying in its simplicity, it is clear that the relations (19) and (20) are at best approximations which will be most realistic when the intensity distribution in the medium approaches the distribution given by equation (12). Many alternatives to the equations (19) are possible. Klier [10] has, for instance, shown that the Kubelka-Munk equations are

formally identical to a class of solutions of the radiative transfer equation for isotropically, highly scattering media. Under this approach the Kubelka-Munk  $s$  and  $k$  may be related to the transfer equation parameters through

$$s = Sf_1 \left( \frac{K}{S} \right), \quad k = Kf_2 \left( \frac{K}{S} \right) \quad (21 \text{ a,b})$$

The nonlinear functions  $f_1$  and  $f_2$  are tabulated in [10]. For weak absorption the reference gives  $f_1 = .75$  and  $f_2 = 2.0$ . Thus, in this case, equation (19) differs from the Klier equations only in the constant coefficient of the scattering coefficient relation.

In the Results and Discussion section, Kubelka-Munk solutions for reflectance, radiative flux and radiative flux divergence are compared with transfer equation solutions using both relations (19) and (21). These solutions are given below:

#### Exact Kubelka-Munk Solution for Finite Thickness

Following Hamaker [8] the exact solution of the Kubelka-Munk equations (with negligible emission) for the half fluxes may be written:

$$q^+ = A(1-\gamma)e^{\sigma y} + B(1+\gamma)e^{-\sigma y}, \quad q^- = A(1+\gamma)e^{\sigma y} + B(1-\gamma)e^{-\sigma y} \quad (22 \text{ a,b})$$

where

$$\sigma = \sqrt{k(k+2s)}, \quad \gamma = \sqrt{k/(k+2s)} = \sigma / (k+2s) \quad (23 \text{ a, b})$$

and  $A$  and  $B$  are determined by the boundary conditions.

For the case of a scattering, absorbing, non-emitting medium with intense, diffuse incident flux  $q^+(0)$  and opaque non-emitting substrate with reflectance  $R_B$ , the coefficients  $A$  and  $B$  are:

$$A = \frac{q^+(0)e^{-\sigma \delta} [\gamma(1+R_B) - (1-R_B)]}{2 \{ [\gamma^2(1+R_B) + (1-R_B)] \sinh(\sigma \delta) + 2\gamma \cosh(\sigma \delta) \}} \quad (24a)$$

$$B = \frac{q^+(0)e^{\sigma \delta} [\gamma(1+R_B) + (1-R_B)]}{2 \{ [\gamma^2(1+R_B) + (1-R_B)] \sinh(\sigma \delta) + 2\gamma \cosh(\sigma \delta) \}} \quad (24b)$$

where  $\delta$  is the thickness of the scattering medium.

This solution is used together with equations (14) to provide an initial radiation field for the numerical iteration of the transfer equation discussed earlier. The Kubelka-Munk net radiative flux and radiative flux divergence may be found by using equation (14c) and eliminating derivatives using the Kubelka-Munk differential equations (18):

$$q = q^+ - q^- \quad (25)$$

$$\frac{dq}{dy} = \frac{dq^+}{dy} - \frac{dq^-}{dy} = -k (q^+ + q^-) \quad (26)$$

The hemispherical reflectance of a layer of infinite thickness,  $R_\infty$ , and of a finite layer may be obtained from (8) and (22) as:

$$R_\infty = \frac{q^-(0)}{q^+(0)} = \frac{1-\gamma}{1+\gamma} = 1 + \frac{k}{s} - \sqrt{\frac{k}{s} \left( \frac{k}{s} + 2 \right)} \quad (27)$$

and

$$R = \frac{(1/R_\infty)(R_B - R_\infty) - R_\infty (R_B - 1/R_\infty) \exp [s\delta (1/R_\infty - R_\infty)]}{(R_B - R_\infty) - (R_B - 1/R_\infty) \exp [s\delta (1/R_\infty - R_\infty)]} \quad (28)$$

#### Approximate Solution for Weakly Absorbing Media

A good volume reflector is characterized by low absorption coefficient and high scattering coefficient. In this situation an existing approximate solution of the Kubelka-Munk equations with negligible emission may be useful. This approach, used in [9], involves solution of the Kubelka-Munk equations for the case of zero absorption coefficient subject to a specified incident diffuse flux and specified overall reflectance. The resulting solutions may be written as:

$$q^+(y) = q^+(0) [1 - sy(1-R)], \quad q^-(y) = q^+(0) [R - sy(1-R)] \quad (29 a, b)$$

This approximation implies that the net radiative flux is given by:

$$q = q^+ - q^- = q^+(0) [1-R] \quad (30)$$

It is evident that in this approximation  $q$  is independent of depth. Using equation (26)

the radiative flux divergence may be approximated by combination with equation (29):

$$(dq/dy) = -k q^+(0) [1+R - 2 sy (1-R)] \quad (31)$$

In these approximations the reflectance  $R$  is evaluated using equation (28). Other suitable approximations may be used however. Note that expressions (29) and (31) are clearly limited on physical grounds to depths for which the terms in brackets are positive.

### RESULTS AND DISCUSSION

When an intense, diffuse radiative flux is incident on a highly scattering and weakly absorbing medium it is well known that an intense, diffuse reflection occurs. The reflected flux, for medium indices of refraction close to one, originates as a result of penetration in depth of the incident rays, rather than as a surface phenomenon. Internally, multiple scattering processes cause a redirection of a large fraction of the incident radiant energy back toward its surface of entry. The ultimate re-emergence of the majority of the incident and scattered photons is made possible by the absence of strong absorption within the medium.

The manner in which energy is redistributed is shown in Figure 2. There the intensity variation with depth is presented for a nonabsorbing, isotropically scattering medium, ( $\omega=1.0$ ), with a black substrate. It is evident that the incident transmitted rays diminish in intensity with depth even in the absence of radiative absorption. This effect is more pronounced as the path length increases ( $\mu_1$  approaches zero). Photons penetrating to the black substrate are absorbed there and new rays emerge directed toward the incident flux boundary. These rays, initially equal in intensity, are augmented in intensity as they progress toward  $\eta = 0$  due to scattering from each of the other rays. Again rays traversing greater path lengths are influenced more by scattering than those closer to the surface normal.

The influence of the substrate reflectance on the dimensionless intensity field is shown in Figure 3 for a weakly absorbing, isotropically scattering medium with negligible emission. The lines and symbols show intensity distributions for substrate specular reflectances of 0 and 0.8 respectively. Comparison of the two intensity families shows clearly

the importance of substrate reflectance even for optical thicknesses of the order of three. The distributions of dimensionless intensity at the incident flux boundary ( $\eta = 0$ ) are also hemispherical-directional reflectance distributions. The monotonic decrease in reflectance toward the outward normal to the incident flux surface is apparent. Evidently the increased scattering influence due to path length discussed above is controlling this distribution.

The influence of quadrature order on the intensity field is demonstrated in Figure 3 also. It is evident that quadrature orders above four are necessary only for filling in the distribution, as has been pointed out elsewhere in a related problem [4].

It is indicated above that the influence of emission from the medium and substrate may be negligible under an intense incident flux. For the incident field considered in Figure 3, corresponding to a black emitter at  $3000^{\circ}\text{K}$ , calculations indicate that the intensity field changes by less than 1.5% when the medium and substrate temperatures are changed from  $300^{\circ}\text{K}$  to  $1000^{\circ}\text{K}$ . Thus neglect of emission is well justified for a large class of dielectric solids at moderate temperatures.

The influence of anisotropic scattering on the internal intensity field is presented in Figure 4 by comparing transfer equation solutions for strong forward scattering ( $x = 1.0$ ) and strong backward scattering ( $x = -1.0$ ) with the isotropic solution ( $R_B = .8$ ) of Figure 3. It is clear that even with this extreme anisotropy the basic character of the distributions is unchanged. It may be observed in Figure 4 that forward scattering reduces the attenuation of incoming rays and that this effect becomes more pronounced with increasing depth. While the substrate-reflected intensity for forward scattering is greater than for the isotropic case, reduced augmentation by scattering into rays directed toward the incident flux boundary produces a lower intensity level emerging from the medium than for isotropic scattering. Thus the medium reflectance is reduced due to forward scattering with respect

to the isotropic case. This may be viewed simplistically as increased trapping of energy due to deeper penetration by forward scattering and due to absorption of this energy in the medium and at the substrate. Conversely for backward scattering less energy penetrates to a given depth to be trapped than for isotropic scattering. As a consequence, more energy is returned to the incident flux boundary in the emerging rays, leading to increased reflectance for backward scattering media. Hemispherical reflectances calculated for each of these cases are tabulated on the figure.

The total diffuse reflectance of isotropically scattering volume reflectors is considered in Figure 5 as a function of albedo, optical thickness and substrate reflectance. Values computed from the Kubelka-Munk reflectance equation (28) show the transition from optically thin to optically thick media for several values of albedo and substrate reflectance. The solid lines show the Kubelka-Munk reflectance interpreted through the relations (19) while the broken lines utilize the Klier relations (21) and the tabular values of  $f_1$  and  $f_2$  from [10]. It is evident that the difference between the two representations grows with decreasing albedo.

Values of hemispherical reflectance based on solutions of the equation of radiative transfer are also presented in Figure 5. In addition to values generated in the present study, published results from Lii and Ozisik [16] for media of finite optical thickness and Giovanelli [17] for semi-infinite media are included. Three of the Lii and Ozisik cases were run for comparison purposes with the present iterative program. Two of these were in agreement to three significant figures using 8th order quadrature and 101 nodes. The third, within 1.4% of the Lii and Ozisik value, ( $\tau_0 = 5.0$  and  $\omega = .95$ ) was rerun for 201 nodes and the results were extrapolated in terms of the reciprocal of the number of nodes. Extrapolation in this way to an infinite number of nodes yields agreement with the Lii and Ozisik value in the fourth significant figure.

The transfer equation solutions must of course be regarded as correct values for the reflectance of the scattering, absorbing medium. The two representations of the Kubelka-Munk solutions both show the same qualitative trends as the transfer equation solutions. Quantitatively, the Kubelka-Munk equations using the relations (21) show better agreement with transfer equation solutions than when equation (19) is used.

### Flux and Flux Divergence

The radiative flux and radiative flux divergence variations with depth are presented in Figures 6 and 7 for the intensity field of Figure 3 ( $R_B = .8$ ). In these figures both representations of the Kubelka-Munk exact and approximate fluxes and divergence are compared with solutions of the transfer equation. The Kubelka-Munk results are seen to be reasonable approximations particularly when the Klier representation [10] is employed. For this particular case ( $\tau_0 = 3.177$ ) the Kubelka-Munk exact and approximate values are equally good. This is fortuitous except near the incident flux boundary. It can be shown that approximate and exact Kubelka-Munk expressions are identical at  $\eta = 0$  and tend to deviate increasingly with depth. In all calculations performed, including several not presented here, Kubelka-Munk divergence values were in excellent agreement with transfer equation values at the incident flux boundary. In view of the limitation of the approximate solutions discussed following equation (31) two additional optical thicknesses are shown in Figure 7. It is evident that both types of Kubelka-Munk solution deteriorate at the highest optical thickness--the approximate solution the more rapidly.

Also shown in Figures 6 and 7 are flux and flux-divergence distributions for the anisotropic cases of Figure 4. The increased penetration of the incident flux and net flux for forward scattering and decreased penetration for backward scattering as discussed above

are evident in Figure 6. Increased energy loss from the radiation field for forward scattering and decreased loss for backward scattering are evident in the corresponding increase and decrease in the divergence distributions in depth in Figure 7.

The influence of the albedo of highly scattering layers on the net radiative flux and on a flux divergence parameter is shown in Figures 8 and 9. It is evident that the Kubelka-Munk exact solutions provide good approximations over the entire range of  $\omega$  considered, particularly when equation (21) is employed. It is also apparent that the Kubelka-Munk approximations are useful only for  $\omega > .995$ . That this is not a fatal limitation is evident from Figure 5 which shows that this range includes optically thick volume reflectors with reflectances as low as .85. The limitation of the approximate divergence equation (31) discussed earlier is apparent in Figure 9. Notwithstanding their limitations, the Kubelka-Munk approximations may be utilized in the study of high performance volume reflecting heat shields.

### CONCLUDING REMARKS

Accurate numerical solutions of the equation of radiative transfer have been developed for the evaluation of approximation methods for reflectance and radiative flux parameters. Convergence and divergence criteria are given for the numerical solution of the system of coupled differential equations used. New hemispherical reflectance values are presented and compared with existing values in the literature. The Kubelka-Munk and Schuster Schwarzschild two-flux theories are obtained as consequences of the equation of radiative transfer under the assumption of directionally independent intensity fields. This approach yields simple linear relations between transfer equation and Kubelka-Munk scattering and absorption coefficients. An alternate interpretation of the Kubelka-Munk theory as an exact theory of an asymptotic solution of the equation of radiative transfer

yields slightly different nonlinear relations between the coefficients. Exact and approximate Kubelka-Munk solutions were compared with exact solutions of the equation of radiative transfer using both interpretations. The exact Kubelka-Munk solutions are found to provide realistic approximations to transfer equation results over a wide range of conditions while approximate Kubelka-Munk relations are applicable over a more restricted range of conditions.

#### REFERENCES

1. Nachtsheim, P. R., D. L. Peterson and J. T. Howe, "Reflecting Ablative Heat Shields for Radiative Environments," American Astronautical Society Preprint AAS-71-147, 1971.
2. Roux, J. A., A. M. Smith and F. Shahrokhi, "Radiative Transfer Properties of High Albedo CO<sub>2</sub> and H<sub>2</sub>O Cryodeposits," AIAA Paper 72-58, 1972.
3. Judd, D. B. Color in Business, Science and Industry, John Wiley and Sons, 1952.
4. Evans, L. B., C. M. Chu and S. W. Churchill, "The Effect of Anisotropic Scattering on Radiant Transport," Journal of Heat Transfer, Trans. ASME, 1965, 87, Series C, (3), 381-387.
5. Hottel, H. C., A. F. Sarofim, L. B. Evans and I. A. Vasalos, "Radiative Transfer in Anisotropically Scattering Media: Allowance for Fresnel Reflection at the Boundaries," Journal of Heat Transfer, Trans. ASME, 1968, 90, Series C, (1), 56-62
6. Chandrasekhar, S., Radiative Transfer, Dover, 1960.
7. Viskanta, R., "Radiation Transfer and Interaction of Convection with Radiation Heat Transfer," Advances in Heat Transfer, 3, Academic Press, 1966.
8. Hamaker, H. C., "Radiation and Heat Conduction in Light Scattering Materials," Philips Res. Rep., 1947, 2, 55-67.
9. Weston, K. C., J. T. Howe and M. J. Green, "Approximate Temperature Distribution for a Diffuse, Highly Reflecting Material," AIAA Journal, 1972, 10, (9), 1252-1254.
10. Klier, K., "Absorption and Scattering in Plane Parallel Turbid Media," Journal of the Optical Society of America, 1972, 62, (7), 882-885.
11. Bergquam, J. B. and R. A. Seban, "Heat Transfer by Conduction and Radiation in Absorbing and Scattering Materials," Journal of Heat Transfer, Trans. ASME, 1971, 93, Series C, (2), 236-239.
12. Hottel, H. C., A. F. Sarofim, I. A. Vasalos, and W. H. Dalzell, "Multiple Scatter:

Comparison of Theory with Experiment," Journal of Heat Transfer, Trans. ASME, 1970, 92, Series C, (2), 285-291.

13. Shahroki, F. and P. Wolf, "Numerical Solution to the Radiation Heat Transfer Equation for Scattering Medium," AIAA Journal, 1968, 6, (9), 1748-1752.
14. Varga, Richard S., Matrix Iterative Analysis, Prentice Hall Inc., 1962.
15. Weston, K. C. and J. L. Hauth, "Unsteady, Combined Radiation and Conduction in an Absorbing, Scattering and Emitting Medium," Journal of Heat Transfer, Trans. ASME, 1973, 95, Series C, (3), 357-364.
16. Lii, C. C. and M. N. Ozisik, "Hemispherical Reflectivity and Transmissivity of an Absorbing, Isotropically Scattering Slab with a Reflecting Boundary," Int. J. Heat Mass Transfer, 1973, 16, 685-690.
17. Giovanelli, R. G., "Reflection by Semi-Infinite Diffusers," Optica Acta, 1955, 2, (4), 153-162.

## LIST OF CAPTIONS

- Figure 1: Convergence Criteria for Numerical Calculations,  $\omega = .9995$ ,  $\tau_o = 3.177$  unless otherwise noted,  $x = 0$ ,  $R_B = .8$ ; Negligible Emission.
- Figure 2: Intensity Field for Isotropically Scattering, Nonabsorbing Medium with Black Substrate.  $\omega = 1.0$ ,  $\tau_o = 1.0$ , Medium Temperature = Incident Flux Temperature =  $1111^\circ\text{K}$ , Substrate Temperature =  $555^\circ\text{K}$ .
- Figure 3: Influence of Quadrature Order on the Intensity Field for an Isotropically Scattering Medium.  $\omega = .9995$ ,  $\tau_o = 3.177$ , Negligible Emission.
- Figure 4: Comparison of Intensity Fields for Isotropic and Anisotropic Scattering.  $\tau_o = 3.177$ ,  $\omega_o = .9995$ ,  $R_B = .8$ , Negligible Emission.
- Figure 5: The Hemispherical Reflectance of Isotropic Scattering Layers Mounted on a Opaque Substrate. Negligible Emission.
- Figure 6: Comparison of Radiative Flux Distributions Calculated from the Transfer Equation and from the Kubelka-Munk Theory.  $\tau_o = 3.177$ ,  $\omega = .9995$ ,  $R_B = .8$ , Negligible Emission.
- Figure 7: Comparison of Radiative Flux Divergence Distributions Calculated from the Transfer Equation and the Kubelka-Munk Theory.  $\omega = .9995$ ,  $R_B = .8$ , Negligible Emission.
- Figure 8: The Influence of Albedo on the Net Radiative Flux at Three Optical Depths.  $\tau_o = 3.177$ ,  $R_B = .8$ ,  $x = 0$ , Negligible Emission.
- Figure 9: The Influence of Albedo on the Radiative Flux Divergence at Three Optical Depths.  $\tau_o = 3.177$ ,  $R_B = .8$ ,  $x = 0$ , Negligible Emission.

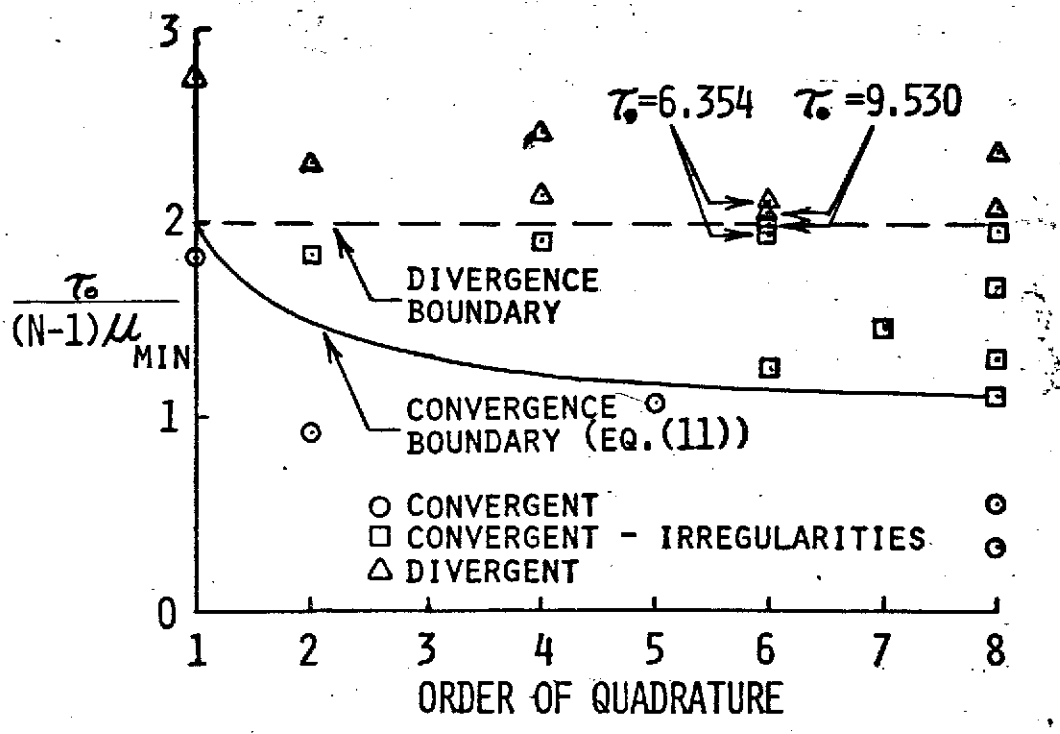


Fig 1

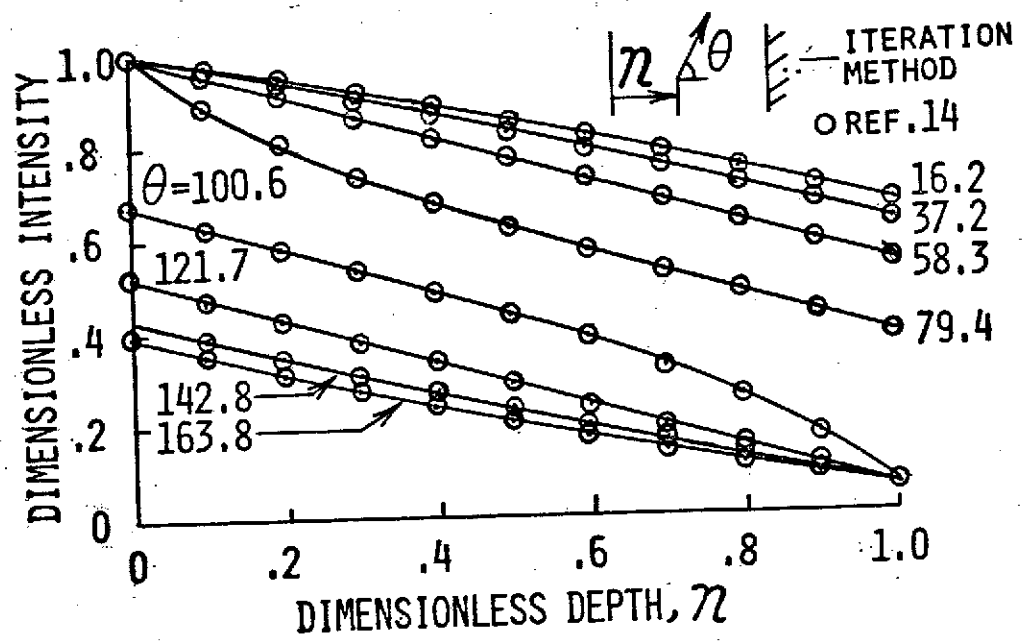


Fig. 2

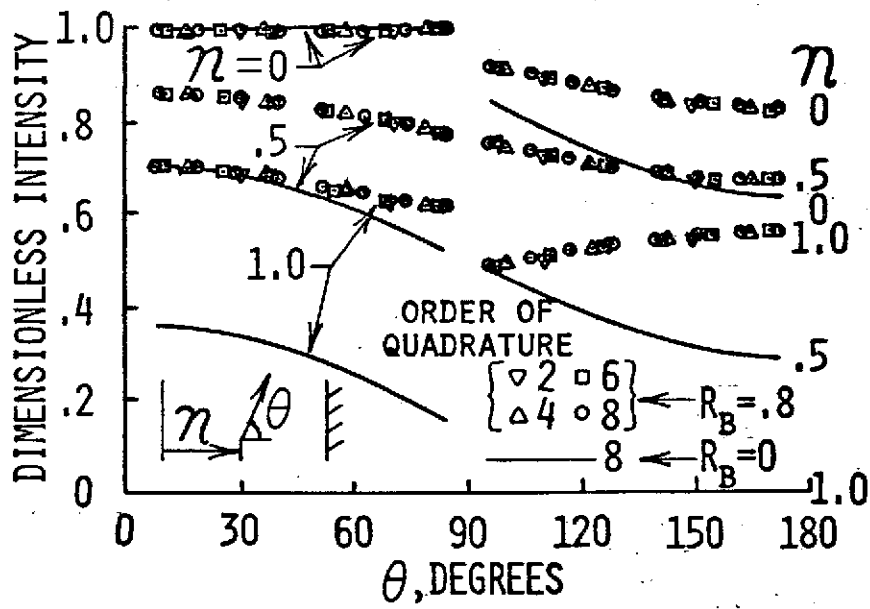


Fig. 3

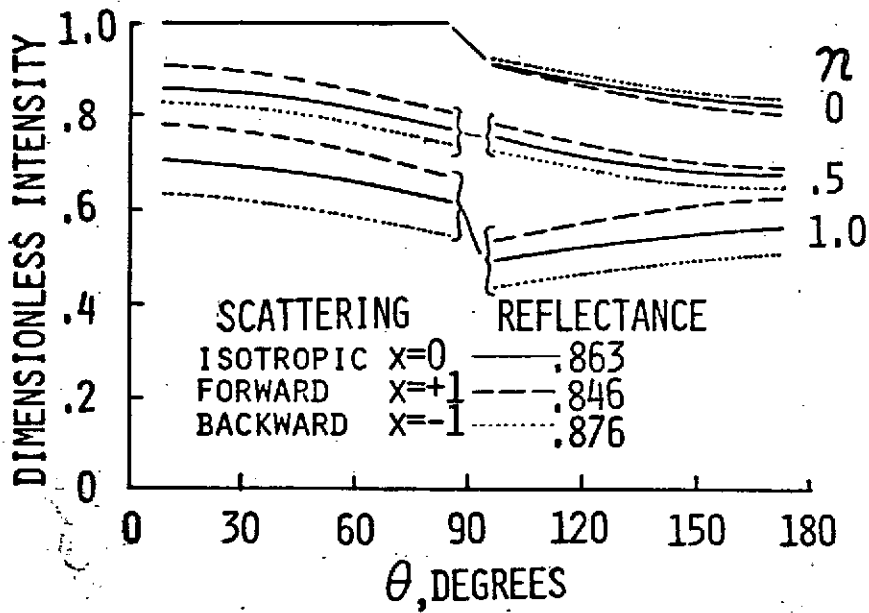


Fig. 4

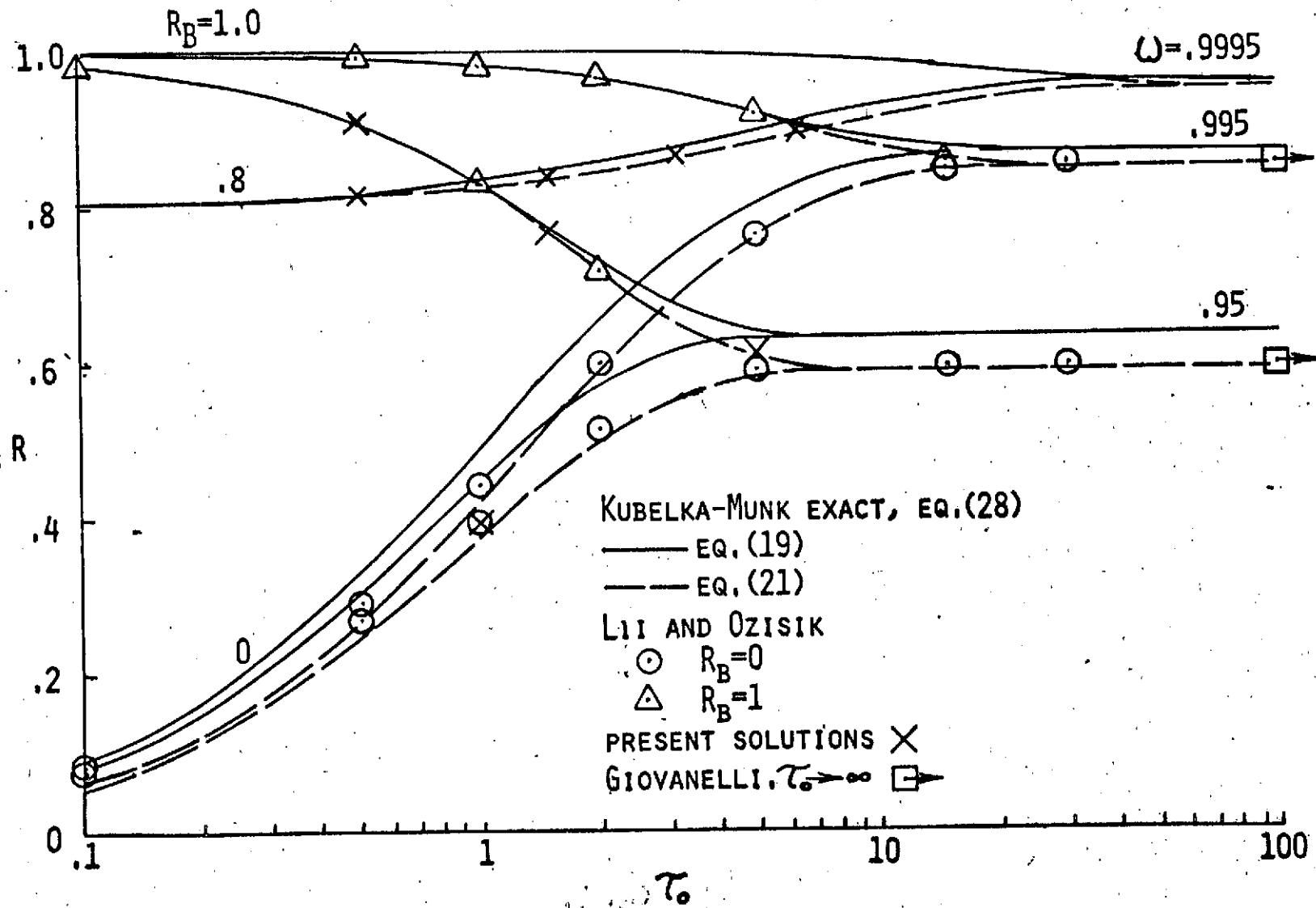


Fig. 5

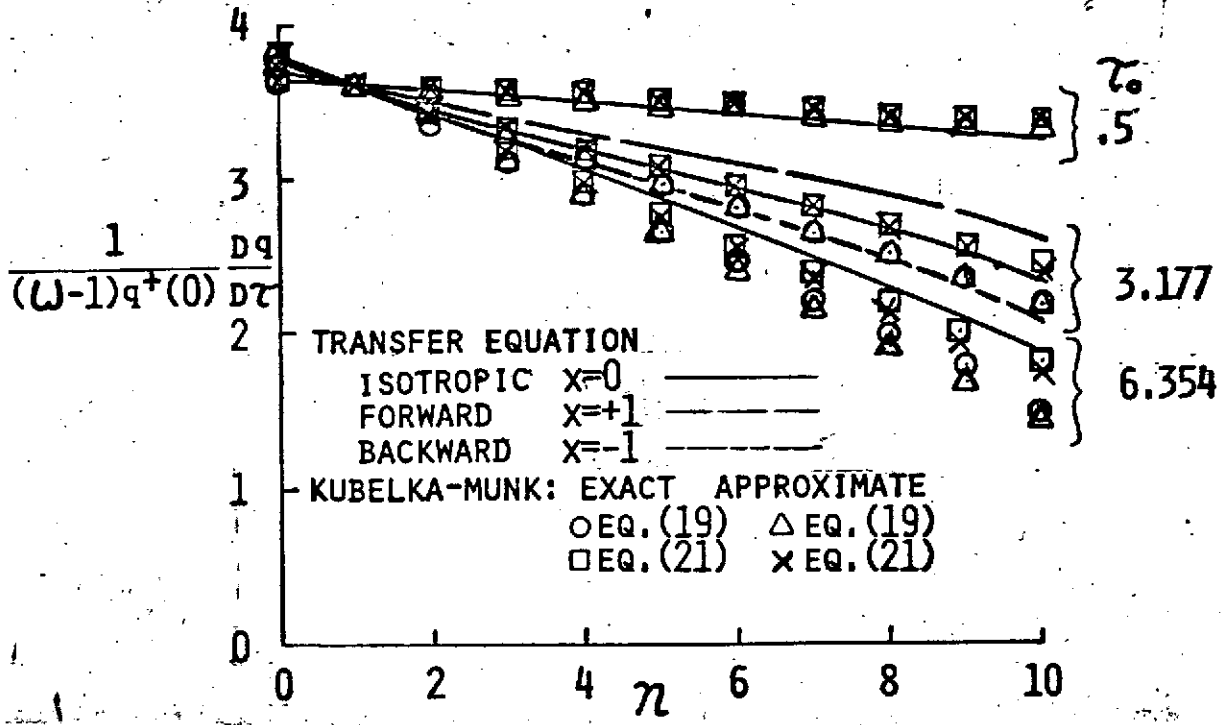


Fig 7

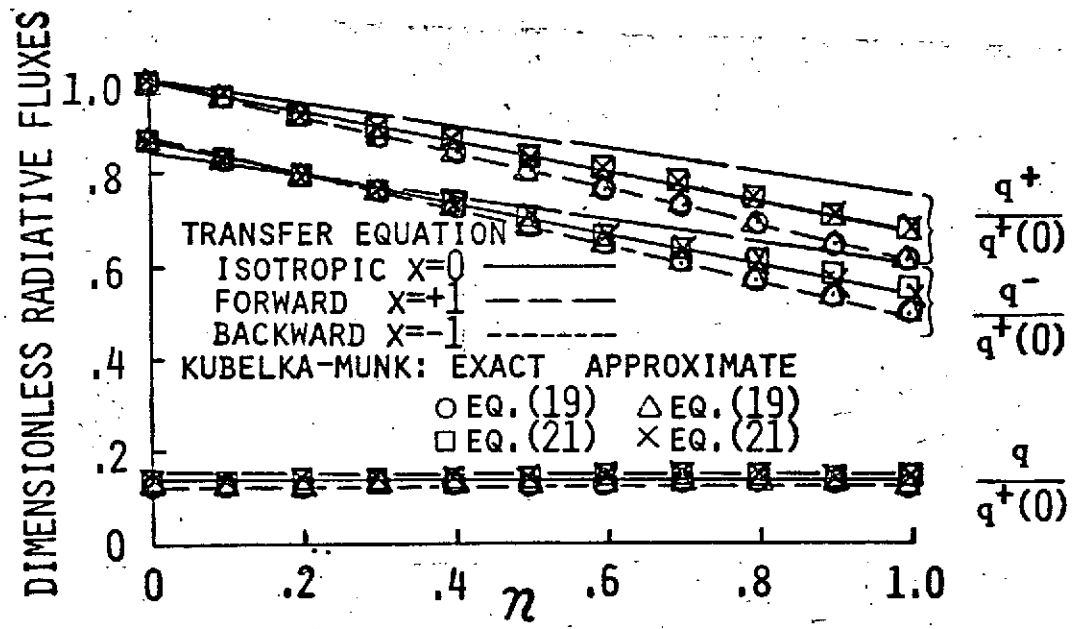


Fig. 6

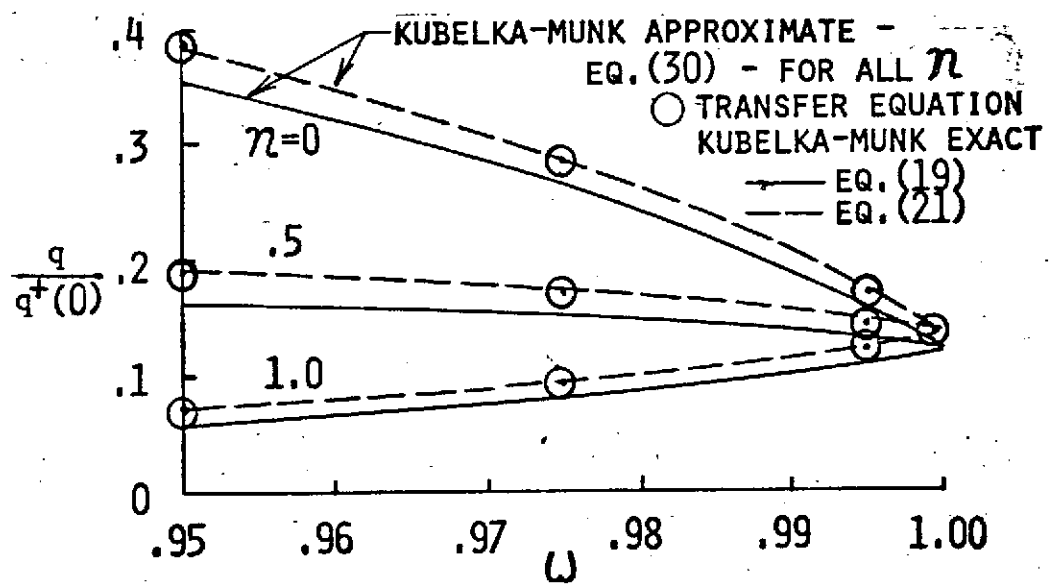


Fig. 8

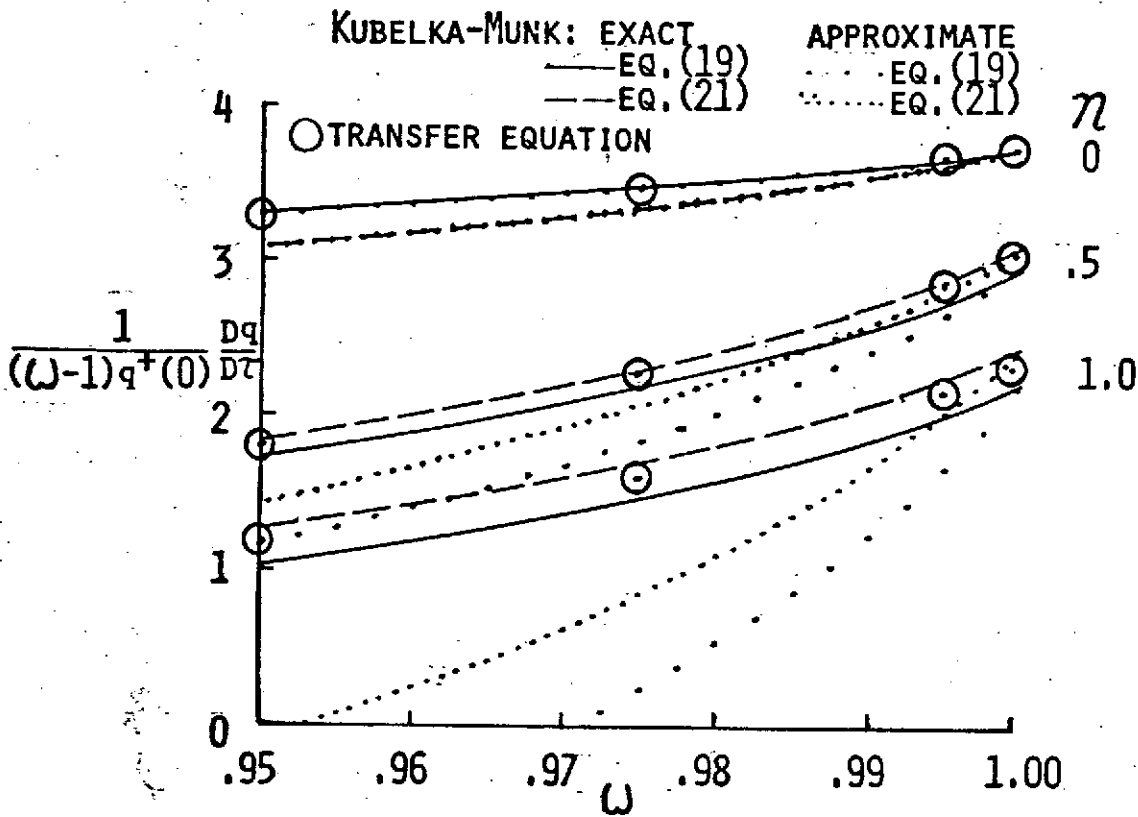


Fig. 9